Hindawi Publishing Corporation
International Journal of Distributed Sensor Networks
Volume 2013, Article ID 315841, 12 pages
http://dx.doi.org/10.1155/2013/315841

*Research Article*

# Personalization in Mobile Activity Recognition System Using $K$-Medoids Clustering Algorithm

**Quang Viet Vo, Minh Thang Hoang, and Deokjai Choi**

*ECE, Chonnam National University, Gwangju 500-757, Republic of Korea*

Correspondence should be addressed to Deokjai Choi; dchoi@jnu.ac.kr

Received 5 February 2013; Accepted 12 June 2013

Academic Editor: Tai-hoon Kim

Nowadays mobile activity recognition (AR) has been creating great potentials in many applications including mobile healthcare and context-aware systems. Human activities could be detected based on sensory data that are available on today's smart phone. In this study, we consider mobile phones as an independent device since sending the data to central server can generate privacy issues. Furthermore, applying AR on mobile phone does not only require an effective accuracy rate but also the lowest power consumption. Normally, an AR model learnt from acceleration data of a specific person is distributed to other people to recognize the same activities instead of generating different models individually. This work often cannot create accurate results on the prediction in broad range of participants. Moreover, such AR model also has to allow each user to update his new activities independently. Therefore, we propose an algorithm that integrates Support Vector Machine classifier and $K$-medoids clustering method to resolve completely the demand.

## 1. Introduction

Currently, mobile-based AR has been applied widely in various technological aspects to enhance the quality of life. In healthcare applications, it has been used to assess physical activities and aid cardiac rehabilitation, detect a fall event as in our achievement [1], predict user's energy consumption based on monitoring activity of daily living (ADL), and generate daily, weekly, and monthly activity reports in order to promote health and fitness. In context-aware pervasive computing systems, mobile accelerometer has gained significant achievements. In term of user's device security improvement, gait recognition is studied as a potential protection mechanism [2, 3]. Moreover, human activity information can also be used to adapt automatically the behavior of using mobile phone. It can include sending calls directly to voicemail if a user is bicycling or jogging, turning on music when jogging is taken place, and so forth. In order to gain these benefits, mobile phone accelerometer data must be processed at device or central server via communication channels (Wi-Fi, Bluetooth, etc.). In this study, we consider mobile phones as an independent device since sending the data to central server from mobile device can generate privacy issues [4]. Normally, there are 3 steps in AR. First, data windows from segmentation of accelerometer signals are taken. Second, some features that describe the clearest properties of studying activity are extracted. These preprocessing steps are the most important parts of AR system since the last step is classification that can be studied by any existing machine learning algorithms.

Some recent mobile achievements attempted to recognize ADL as in [5, 6]. However, these achievements also remain restrictions including the instability of accuracy especially in cross-people prediction which measures the sustainability of classification features in predicting activities of new people based on a trained model from a specific person and lacking of evidence about energy consumption since mobile devices are powered by limited energy resource and memory storage. To resolve these problems, in our latest studies [7, 8], we proposed (1) an effective classification feature extraction to balance accuracy and energy consumption and (2) an adaptive strategy for energy saving by selecting appropriately the combination of feature classification (CF) and sampling frequency (SF) for each activity.

From our previous achievements, classification models were created offline from the training data and ported to different mobile users to measure the tolerance of the classification. However, in fact it is hard to generate a unique model that can classify all users' motion activities in a large scale of participants.

This issue was denoted in our previous achievement as in Figure 1. The overall accuracy descended significantly when we increase the number of subjects. Moreover, an effective mobile AR system should allow users to update their own new activities instead of only predicting predefined activities. Addressing these needs, we propose an algorithm to achieve the following goals:

(i) enhancing the personalization in mobile AR system for predefined activities based on the actual data of its owner;

(ii) allowing new activities that are updated on each mobile user.

Applying AR on mobile phone is not like applying on power machine. It not only requires effective accuracy but also guarantees the lowest power consumption. Therefore, we propose the following methods.

(i) Firstly, we propose an effective real-time mobile AR system. Its preprocessing phase includes motion analysis on $Y$- and $Z$-axes from mobile triaxial accelerometer and segmenting on main $Y$-axis based peak detection algorithm. Proposed classification features in each window are extracted in time domain. Section 3 presents this core system.

(ii) A personalization algorithm is presented through the method that selects confident samples to update the existing model. The proposed algorithm is integration of SVM classifier and clustering algorithm. In this study, clustering algorithm is aimed to explore two common partitioning methods—$K$-means [9] and $K$-medoids [10]. Section 4 presents our personalization method.

ADLs in this study include walking, jogging, bicycling, going upstairs and downstairs, and running while the phone is attached at front pant pocket of mobile user. Experiments of our two main contributions are presented in Sections 5 and 6, respectively. Finally, Section 7 gives our conclusion.

## 2. Related Works

A few recent AR achievements, like ours, did use a commercial mobile accelerometer to measure real-time running capability of mobile phone without sending data to central server. The authors in [11] achieved 75.3% and 73.95% in walking, jogging, upstair, and downstair activities by using J48 and Multilayer Perceptron. By using iPhone accelerometer, the authors in [12] predicted walking, running, biking, and driving activities with average accuracy to reach 93.88% by using SVM. However, driving is similar with relaxing activity which does not have significant changes in acceleration. Therefore, prediction becomes easier. Other authors in [5] had restrictions in detecting upstairs and downstairs activities.

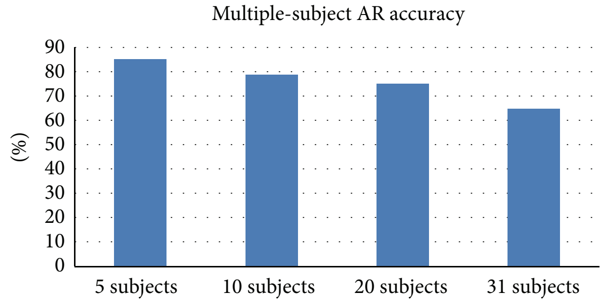

Figure 1: Accuracies of mobile AR system in multiple-subject prediction type on SCUT-NAA dataset in our achievement [8].

According to on-board training on mobile phone as the classification model is created individually on every user [11, 13], this approach can allow users update their own new activities. However, a sufficient training sample quantity must be collected on each phone user that could cause unexpected inconvenience. Thus, an implicit method that allows personalization on predefined activities and updating new activities is necessary in user's mobile AR system.

Based on transfer learning technique [14], personalization issue was also recently studied on mobile [15]. In this approach, $K$-means is used to select confident samples, and the convergence of personalized model comes from comparing parameters inside the model at two continuous iteration steps. In our solution with another approach, the equality of confident samples at the steps is considered as a stopping condition in the personalization phase. With the core SVM classification, we measure the performance of clustering methods among the $K$-means and $K$-medoids through the presented targets.

In our study, the targets are denoted as in Figure 2. Model A is generated from user A's data on specific activities. The model is then distributed to other users with essential demands including personalizing these activities and updating new activities for each user independently.

## 3. Mobile AR System Based on Gait Cycle

In this study, we paid particular attention to front pant pocket because of the popularity of attaching phone at this position. The mobile phone was vertically placed at the pocket location as shown in Figure 3. From three axes of accelerometer, the $X$-axis captures horizontal movement of the user's leg. The $Y$-axis captures the upward and downward motion; the $Z$-axis captures the forward movement.

*3.1. System Overview.* A flowchart of the proposed mobile AR method is depicted in Figure 4. Only effective axes of mobile accelerometer that presents the most clearly gait cycles in human motion are used. A set of features is extracted on time domain after passing preprocessing steps. SVM classification is used in our core system.

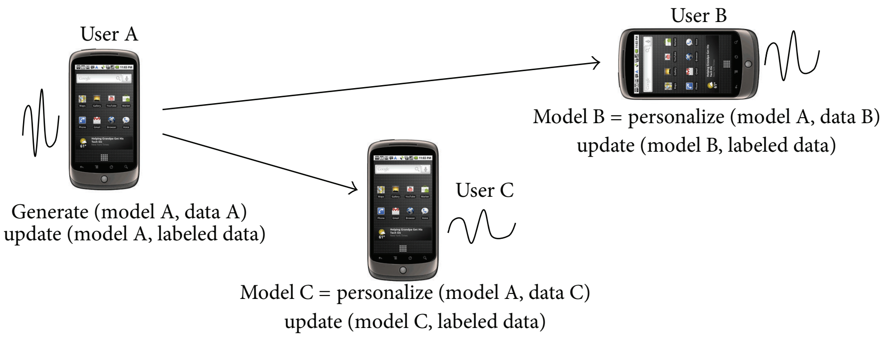
User A
User B
User C
Generate (model A, data A)
update (model A, labeled data)
Model B = personalize (model A, data B)
update (model B, labeled data)
Model C = personalize (model A, data C)
update (model C, labeled data)

Figure 2: Distribution model A to users and demands of personalization and updating new activities.

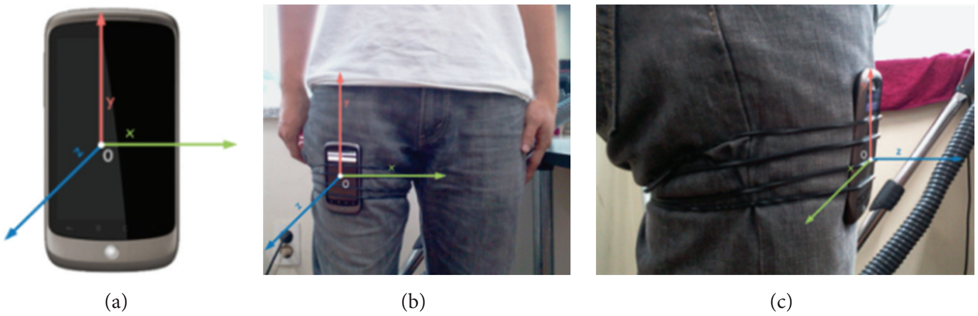

Figure 3: 3-D coordinate of accelerometer and phone attached to the trouser pocket position.

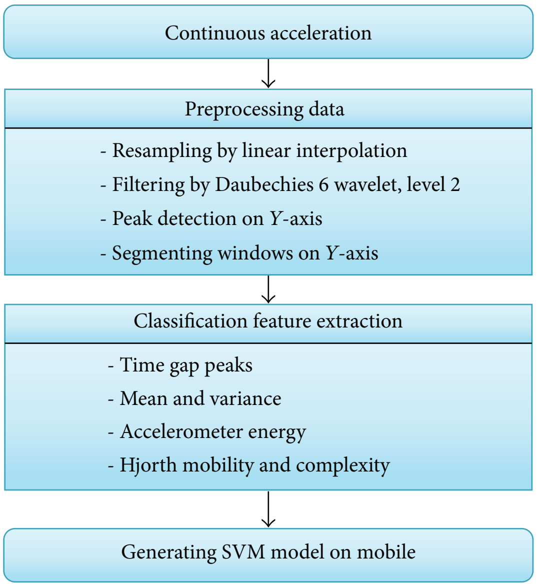
Continuous acceleration
Preprocessing data
- Resampling by linear interpolation
- Filtering by Daubechies 6 wavelet, level 2
- Peak detection on Y-axis
- Segmenting windows on Y-axis
Classification feature extraction
- Time gap peaks
- Mean and variance
- Accelerometer energy
- Hjorth mobility and complexity
Generating SVM model on mobile

Figure 4: A Proposed method for real-time mobile AR system.

*3.2. Effective Axis Selection.* Gait cycle notion is used to explain the combinative force that is recorded by mobile accelerometer. The notion is defined as the time interval between two successive occurrences of one of the repetitive events when walking. In other words, two consecutive steps form a gait cycle. As shown in Figure 5, the cycle starts with initial contact of the right toe, then it will continue until the right toe contacts the ground again. The left goes through exactly the same series of events as the right, but displaced in time by half of a cycle.

When the toe touches the ground in phase "a" or phase "g" as in the figure, the association between ground reaction force and forward inertial force together makes the $Z$-axis signal strongly changes and forms peaks with the high magnitude. In fact, in order to make changes of $Z$-axis we need the change of $Y$-axis beforehand since heel touches the ground. It explains why we always have peaks of $Y$- and $Z$-axes like negative peak, and positive peak respectively, as illustrated in Figure 6.

From our observation, we realized that ground reaction force is expressed most clearly especially in jogging and upstair, downstair activities by negative peaks. Therefore we consider $Y$-axis signal as the main axis. The first window segmentation is started by the first peak on $Y$-axis instead of choosing first point of the window. This reflects clearly properties of activities since it shows how many peaks existed in one window so that it enhances accuracy in matching method. In overlapping of windows, a next window is still started at a peak which occurred in previous window.

Other values on $Z$-axis are just selected at the same time with $Y$ values. A gait cycle is defined between two consecutive peaks on $Y$-axis.

In previous studies [5, 6, 11, 16], windows can be segmented from arbitrary points which only guarantee the length of the window. This might cause an incorrect reflection of human activities on each gait cycle. Thus, the segmentation method based on $Y$ peaks is used in our study to extract clearly gait cycle's features.

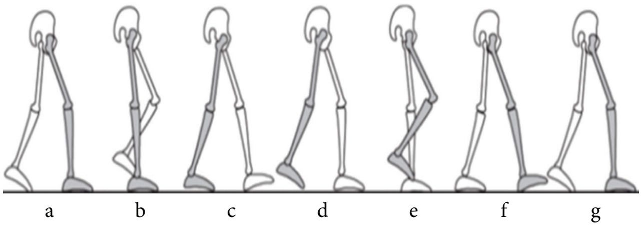

Figure 5: An illustration of a gait cycle.

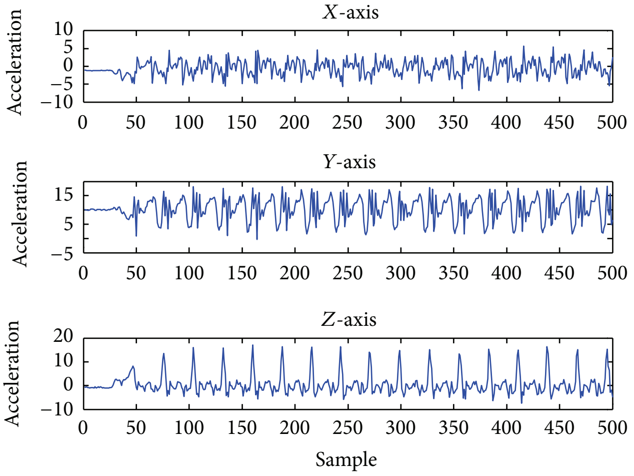

Figure 6: Amplitude in $X$-, $Y$-, and $Z$-axes.

*3.3. Linear Interpolation.* Due to power saving function and the built-in nature, an accelerometer on mobile phone is simpler than standalone one. The sampling rate is rather low. Time intervals between two consecutive acceleration values are also not equal. A sensor only generates value when the forces acting on each axis have a significant change. Therefore, we interpolated the acquired signal to 32 Hz (Figure 7) using linear interpolation method to ensure that the time interval between two sample points will be fixed.

*3.4. Noise Elimination.* When accelerometer samples movement data by user walking, some noises will inevitably be collected. These additional noises could have come from various sources (e.g., idle orientation shifts or bumps on the road while walking). A digital filter needs to be designed to eliminate noises. Multilevel wavelet decomposition and reconstruction method are adopted to filter the signal.

According to Figure 8, original signal is denoted by $S(n)$. High-pass filter and low-pass filter are denoted by HF and LF. On each level, the outputs from high-pass filter are known as detail coefficients. On the other hand, low-pass filter outputs contain most of the information of the input signal. They are known as coarse coefficients. The signal sample is down by 2 at each level. Coefficients obtained from the low-pass filter are used as the original signal for the next level and continue until the desired level is achieved. In contrast, reconstruction is the reverse of decomposition process. To eliminate noises, we assign the detail coefficients to 0. The reconstruction of the signal is computed by concatenating the coefficients of high frequency with low frequency. During experiment, the Daubechies orthogonal 6 wavelet (Db6) is adopted for signal decomposition and noise reduction. Figure 9 showed the signal after noise reduction using Db6 at level 2.

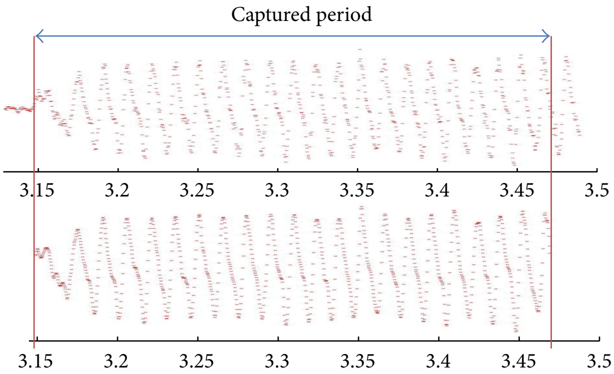

Figure 7: Before and after using linear interpolation into 32 Hz on $Y$ axis.

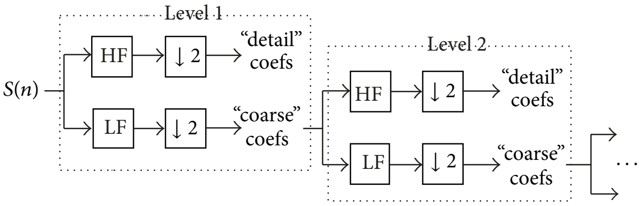

Figure 8: Multi-level wavelet decomposition.

*3.5. Peak Detection Algorithm.* In order to segment window based on $Y$ axis peaks, we designed an algorithm to detect these peaks as follows.

The original signal is denoted as $S(n)$. First, we extract a set of peaks $P$ from $S(n)$. A data point is called peak if its value is less than its previous and next one. Let

$$P = \{d_i \mid d_i < d_{i+1} \wedge d_i < d_{i-1}\} \quad \text{with } i \in [1 \cdots n], \tag{1}$$

where $d_i$ is the $i$th value in $S(n)$. Threshold $T$ is estimated to determine true peaks using (2). The peaks which have magnitudes lower than $T$ are identified as set of true peaks $R$:

$$T = \mu - k\sigma, \tag{2}$$

$$R = \{d_i \in P \mid d_i \leq T\}, \tag{3}$$

where $\mu$, $\sigma$ are mean and standard deviation of all peaks in $P$, respectively, and $k$ is the user-defined constant. Figure 10 shows the threshold $T$ with different $k$ values. In our experiment, choosing $k = 1/3$ gave the best partition rate.

*3.6. Classification Feature Extraction.* Features in our proposed method are extracted in time domain. Each window is segmented by a 256-sample length and the overlapping of 128 data points between consecutive windows. First window is started at the first peak on $Y$ axis in a specific analyzing period of continuous acceleration data.

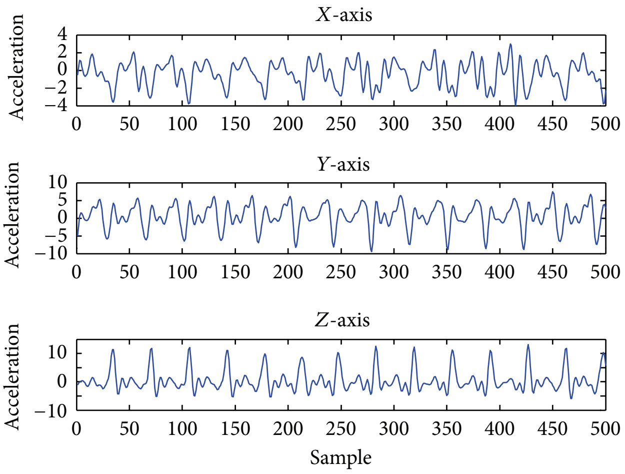

Figure 9: 3-D acceleration after noise reduction.

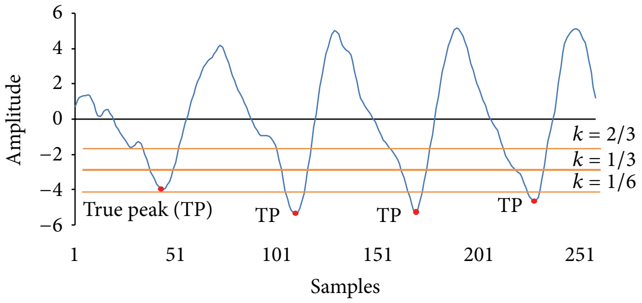

Figure 10: Illustration of true peaks $R$ and the thresholds $T$ with various $k$ values on $Y$ axis.

The following time features (TFS) on sliding windows are chosen in order to record the most clearly gait cycles on each window. They are extracted on effective $Y$- and $Z$-axes, and this is different from [6, 11, 16] since these achievements used features on all axes.

(i) *Time Gap Peaks*. An average value is computed between two consecutive peaks. This value is only computed on main $Y$ axis.

(ii) *Mean and Variance Acceleration*. Mean value is a numerical average of the acceleration values. Variance value shows the mount of variation of the values in the same window.

(iii) *Accelerometer Energy*: This value was also introduced in [5, 17]. Since sampling frequency rate was stable by using linear interpolation, this energy value shows amount of the change on a physical activity. Its value has a significant difference among activities like changes in jogging occurred in both of $Y$- and $Z$ axes but the concentration only focuses on $Y$ axis in bicycling. Equation dedicating it in a window size $T$ is presented as

$$E = \int_{t=t_0}^{t_0+T} |a_x| \, dt, \tag{4}$$

where $a_x$ is acceleration at time $t$ on $Y$- or $Z$-axis.

(iv) *Hjorth Mobility and Complexity*. In electroencephalography (EEG) signal analysis, Bo Hjorth [18] derived certain features that describe the EEG signal by means of simple time domain since this signal cannot be associated with the sine function used in frequency domain. These parameters, namely, Activity, Mobility, and Complexity, were used to characterize the EEG pattern in terms of amplitude, time scale, and complexity. These values were applied in [5, 19] for emotion assessment and also in accelerometer, respectively. Mobility is a measure of the signal mean frequency. Complexity measures the deviation of the signal from the sine shape. Both values are scalar features performed as follows with var($x$) being variance function of signal $x$ and $x'$ standing for the derivate of signal $x$:

$$\text{Mobility}(x) = \sqrt{\frac{\text{var}(x')}{\text{var}(x)}},$$
$$\text{Complexity}(x) = \frac{\text{Mobility}(x')}{\text{Mobility}(x)}. \tag{5}$$

From analyzed TF features, our classification is acted by using SVM classifier which is used widely in AR [5, 16]. SVM algorithm is set of support vectors which separate training samples to a corresponding class by maximizing margin of hyperplanes among classes. In this work, we use Radial Basis Function (RBF) kernel in order to map support vectors to multiple dimensions since there are eleven TF attributes.

## 4. Personalization in Mobile AR System

An AR model is firstly trained offline on power machine by actual mobile acceleration data on known activities of a specific person through the proposed feature extraction. Personalization on mobile AR system in our method is studied on two phases. Firstly, the system has to allow users to update their own new activities. Secondly, in the context of sharing the trained model, the system has to update implicitly and suitably activities trained on that model. This is to predict accurately activities of new users since each person has different ranges in data distribution.

*4.1. On-Board Training Undefined Activities.* Generating individual model for each person causes a large data acquisition and inconvenience for mobile users in reality. Thus, as the simulation shown in Figure 2, the phone on person B uses the model $M_A$ of user A to predict his own activities. A new activity $A_i$ with its label $j$ which has not yet been defined inside the model can be updated directly on mobile based on labeled samples of the activity. Consider

$$M_A = \text{update}(M_A, x_{\text{tar}}, j), \tag{6}$$

where $x_{\text{tar}}$ is extracted feature set of a sample of $A_i$. This function simply increases predicting new activities of person B on the model through on-board updating on his phone.

*4.2. Improving Personalization in Predefined Activities.* In the scope of a small user group, a user's trained model could recognize the data of other people with acceptable accuracy rates. However, in fact, it is hard to generate an effective model that can classify all users' motion activities in a large quantity of participants; this means that the trained model is not sustainable for a really new person because of the different data distribution among participants. Thus, the solution of taking an effective amount of unlabeled data of person B for personalizing not only makes more convenience but also enhances prediction ability for those who use this model instead of keeping fixed accuracy.

With activities trained on $M_A$ from user A, updating $M_A$ by samples of these predefined activities from user B can increase the probability of false-positive rate; therefore personalization means reconstructing parameters of the model to improve the true-positive probability in prediction without expanding data distribution of these activities.

Our solution for this issue is combining an effective clustering algorithm and SVM classifier together. Firstly, we build model A with labeled samples of person A. The model is then transferred to person B's phone. Secondly, we classify the unlabeled samples of person B to model A. These data are then used to adjust model B based on choosing confident samples for updating model A. These steps are represented as in Figure 11.

In the first step, user B's samples $x_{\text{tar}} = \{x_1, x_2, \ldots, x_n\}$ with their corresponding label $j$ could be recognized inaccurately by the original SVM model $M_A$ of person A, where $x_n$ is $n$th attribute of $x_{\text{tar}}$. Consider

$$\text{label}\left(x_{\text{tar}}, M_A\right) = \begin{cases} j & \text{if } D\left(A_{A_j}\right) \sim D\left(B_{A_j}\right), \\ i & \text{with } i \neq j, \end{cases} \tag{7}$$

where $D$ function represents data distribution of activity $A_j$ on each person. The merit of SVM algorithm is performed by maximizing margin of hyper-planes among classes. When samples of activity $A_j$ of person A and B are similar and exclusive from other activities, their hyper-plane can be separated easily in $M_A$ from others. In fact with randomly selecting participants A and B, $D(A_{A_j})$ covers $D(B_{A_j})$ and closes with $D(A_{A_k})$, where $k \neq j$. It involves increasing of false-positive rate as the result $i$ from (7).

In second step, clustering algorithm is a division of samples into group of similar objects. Objects possessed by the same cluster tend to be similar from their feature set $\{x_1, x_2, \ldots, x_n\}$, while dissimilar objects are covered by different clusters. In fact, activity $A_j$'s samples on person B are similar and they perform a unique motion style which is different from other activities [20]. Clustering into groups based on feature space $\{x_1, x_2, \ldots, x_n\}$ performs actual activities of person B. Among clustering methods, we study on two common methods—$K$-means and $K$-medoids—for measuring real-time running capability on mobile device. A clustering method creates $k$ partitions, called clusters, from given set of $n$ data objects. In our study, the dissimilarity between two objects is measured by using Euclidean distance as

$$d_2\left(x_{\text{tar1}}, x_{\text{tar2}}\right) = \left(\sum_{n=1}^{d}\left(x_{\text{tar1},n} - x_{\text{tar2},n}\right)^2\right)^{1/2}. \tag{8}$$

Each partition is represented by either a centroid or medoid. A centroid $\mu_j$ is an average of all data objects in a partition as in (9), while medoid is the most representative point of a cluster [21]. An iterative relocation technique is used to improve the partitioning by moving objects from one group to another. Consider

$$\mu_j = \frac{\sum_{i=1}^{|V_j|} x_i^j}{\left|V_j\right|}, \tag{9}$$

where $V_j$ and $x^j$ denote $j$th class and its samples, respectively. For both of the two methods, clustering quality and iteration number are related to the initial $k$ cluster centers relied on the fact that the new user B has known the number of output classes from $M_A$ before personalizing. In each cluster, $N$ samples which are nearest to their center point are selected since they perform the convergence based on the inner relation of samples in the same cluster. Labels of these samples are then updated by activity label $j$ of the center point. In $K$-means method, the center point is assigned by the sample defined as

$$CP = \min d_2\left(x_{\text{tar}}, \mu_j\right) \quad \text{with } \forall x_{\text{tar}} \in V_j. \tag{10}$$

These confident samples are used to update model $M_A$. Our proposed algorithm is summarized as the following in case of $k = 5$, which means that $M_A$ has five activities on person B; see Algorithm 1.

At step (1), model $M_A$ that was trained based on time domain features of user A is transferred to new user B. From step (3) to step (5), unlabeled samples of user B are classified and clustered based on the parameters including $k$, $\Delta_{\text{Time}}$, and $N$ number defined before. At step (6), confident samples from each class are selected to update $M_A$ with label of their center point. The personalized model for user B is returned when there exists the convergence in *Confidence_Sample* or the excess $\Delta_{\text{Time}}$.

## 5. Experiment Results in Mobile AR System Based Gait Cycle

SCUTT-NAA dataset [16] and our self-constructed data are used in our experiment to measure the efficiency of our real-time AR mobile system and personalization algorithm.

*5.1. With SCUT-NAA Dataset.* SCUTT-NAA dataset contains 1,278 samples from 44 subjects. It was collected from ADXL 330 Accelerometer and sampling frequency is 100 Hz. Because of the limitation of activities in our study, the dataset only provides fully in 31/44 subjects. Each subject experimented two times. In preprocessing phase, some last data points in each experiment time of these subjects were

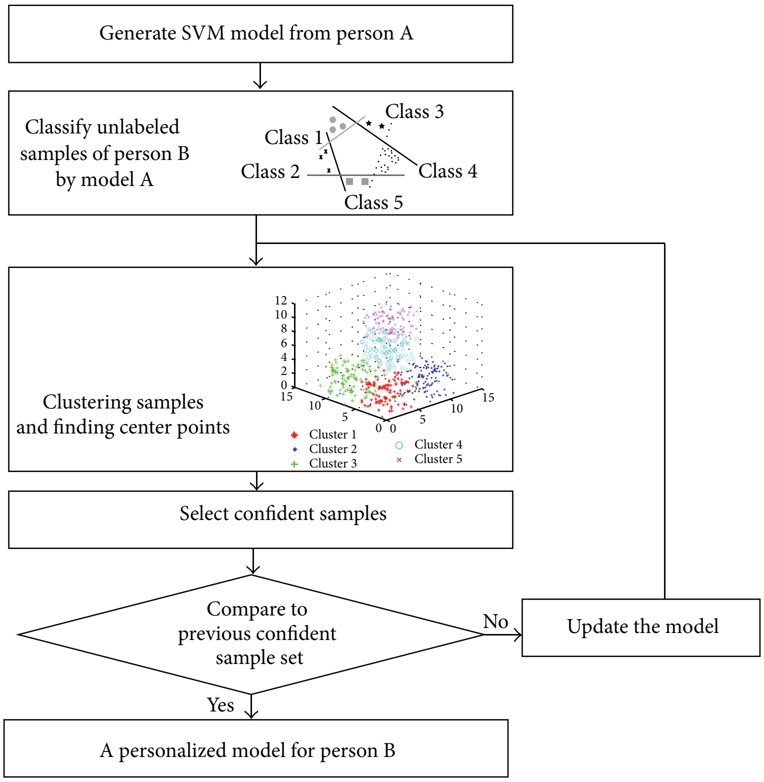
Generate SVM model from person A
Classify unlabeled samples of person B by model A
Class 1
Class 2
Class 3
Class 4
Class 5
Clustering samples and finding center points
12
10
8
6
4
2
0
15
10
5
0
0
5
10
15
Cluster 1
Cluster 2
Cluster 3
Cluster 4
Cluster 5
Select confident samples
Compare to previous confident sample set
No
Update the model
Yes
A personalized model for person B

Figure 11: Our algorithm for personalizing on predefined activities.

removed because these points almost could not present clearly a specific activity's change. Moreover, since our noise elimination step requires a $2^n$ sample length, we firstly shorten the length of each sample to satisfy the conditions in Table 1.

After that, a Daubechies level 3 filter is applied in this step to gain certain information in the change of each activity. Next, peaks on $Y$ axis are detected to segment windows. In this dataset, we found that positive $Y$ peaks could describe more clearly than negative peaks on the same axis. As our best analysis, this phenomenon can be explained such that the author of this dataset placed accelerometer's direction different from our built-in mobile accelerometer. Therefore, our peak detection algorithm is changed a little bit including replacing (1), (2) and (3), respectively, as follows:

$$P = \{d_i \mid d_i > d_{i+1} \wedge d_i > d_{i-1}\} \quad \text{with } i \in [1 \cdots n],$$
$$T = \mu + k\sigma, \tag{11}$$
$$R = \{d_i \in P \mid d_i \geq T\}.$$

Moreover, the interval between true two consecutive peaks has to be greater than 29 data points. We did not choose overlapping method on sliding windows since there was a large data length in each activity of subjects. We separate 512 samples per window. Each window is started from a $Y$ axis peak which is the nearest peak to the last one of previous window. LIBSVM was used to train and predict activities in the dataset and our data.

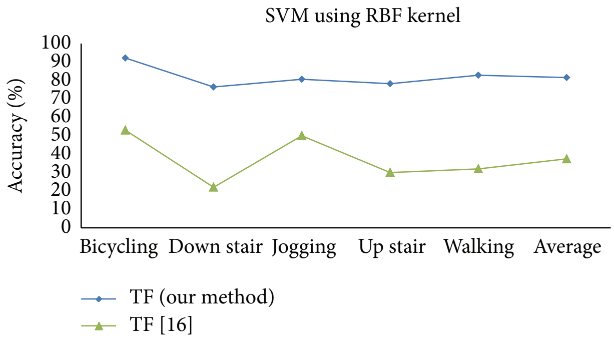

Figure 12: Accuracies in our prediction and Xue and Jin [16].

Table 1: Original and corresponding refined lengths.

| Original length | Data points removed | Refined length |
|---|---|---|
| [0, 4000] | 500 | 2048 |
| [4000, 10000] | 1000 | 4096 |
| Over 10000 | 2000 | 8192 |

Figure 12 shows overall accuracy from our four methods and Xue and Jin [16]. By using SVM with RBF kernel, our TF method shows stable accuracy in predicting the activities. Our contribution in this work is expressed by removing last points in data, selecting effective $Y$- and $Z$-axes without using $X$-axis, selecting different filter, and segmenting windows from peaks on main $Y$-axis. To the best of our knowledge,

```
(1) $D_{\text{tar}} = \{(x_{\text{tar}})\}$; $Activity\_Table = \{A_1, \ldots, A_5\}$; $P_{\text{tar}} = null$; $k = 5$;
    $load(M_A \leftarrow SVM_{TF})$; $t \leftarrow 0$; $Confidence\_Sample = null$;
(2) while $t < \Delta_{\text{Time}}$ do
(3)   $classify(D_{\text{tar}}, M_A)$; $P_{\text{tar}} = \{(x_{\text{tar}}, A_i)\}$;
(4)   $cluster\ (P_{\text{tar}}, k)$;
(5)   $distance((x_{\text{tar}}, A_i), \text{centroid}_{(x_{\text{tar}}, A_i)})$;
(6)   For each cluster, find $N$ samples $(x_{\text{tar}}, A_i)$ where $d(x_{\text{tar}}, A_i)$ are
          closest to its center point.
          Update label $A_i$ of $(N - 1)$ samples by label of center point
          Add these data to Confidence_Samplelist
End For
(7)       if$(Confidence\_Sample_{t-1} \neq Confidence\_Sample_t)$
$update(M_A, Confidence\_Sample)$;
$t = t + 1$;
(8)       else break;
(9) end while
```

Algorithm 1: AR personalization algorithm. New sample $(x_{\text{tar}})$ from a new user which does not have any target class is used to train a learnt model $M_A$ of user A. *Activity_Table* contains all activities in the experiment $\{A_1, \ldots, A_5\}$. $D_{\text{tar}}$ is the set of $\{(x_{\text{tar}})\}$. $P_{\text{tar}}$ is set of labeled samples after classifying by $M_A$. $\Delta_{\text{Time}}$ is the user-defined threshold for iterations. $K$ is the number of high confidence samples selected from clusters from clustering algorithm. Let $N = K/5$. $N$ is number of confidents samples in each cluster. *Confidence_Sample* is list of $(x_{\text{tar}}, A_i)$ samples with $length(Confidence\_Sample) = K$. Output of the algorithm is a personalized model.

Table 2: Number of samples per user and activity.

| ID | Activity training (T) and predicting (P) | | | | | | | | | |
|---|---|---|---|---|---|---|---|---|---|---|
| | Bicycling | | Down stair | | Jogging | | Up stair | | Walking | |
| | T | P | T | P | T | P | T | P | T | P |
| 1 | 30 | 34 | 18 | 12 | 24 | 18 | 18 | 12 | 42 | 30 |
| 2 | 26 | 21 | 12 | 12 | 24 | 18 | 12 | 12 | 60 | 36 |
| 3 | 26 | 28 | 24 | 24 | 24 | 24 | 24 | 24 | 36 | 36 |
| 4 | 28 | 27 | 24 | 24 | 24 | 24 | 24 | 24 | 35 | 36 |
| 5 | 28 | 30 | 30 | 36 | 30 | 30 | 30 | 36 | 30 | 30 |
| 6 | 32 | 30 | 26 | 26 | 24 | 24 | 26 | 26 | 46 | 50 |

this is a novel approach to predict accurately ADL activities based on mobile accelerometer.

*5.2. With Our Self-Constructed Data.* In order to ensure running successfully in real-time environment on mobile accelerometer, we also develop an application for collecting data from triaxial BMA 150 accelerometer on Google Android HTC Nexus One from six volunteers. The mobile device measures acceleration force up to ±2G. The sampling rate is approximately 30 Hz on SENSOR_DEPLAY_FASTEST mode in Android SDK. The data were collected at normal speed of each subject in natural environment. Table 2 shows the numbers of training and predicting data of each activity.

In our data, we used Daubechies at level 2 as noise filtering. Distance between consecutive peaks has to be greater than 23 data points. From the proposed method, our overall accuracies in single and multiple-subject types are shown as in Table 3. The overall accuracies express our contribution in preprocessing phase of mobile AR system based on gait cycles. They guarantee an effective prediction and improve the precision of achievements presented in Section 2.

*5.3. Efficiency in Real-Time AR on Mobile Users.* To measure the performance of our system in real-time running on mobile, we developed two prototypes for this experiment. First prototype uses the proposed method which extracts features in time domain, and the remaining is implemented by using classification features in frequency domain. Public libraries including Android 2.3 OS, Jtransforms, LibSVM, and Weka are used inside these prototypes. Since mobile accelerometer does not collect data when the screen is turned off, our prototypes are developed as a foreground service. Other functions including wireless, light screen were turned off during the experiment. We also developed a power measurement module based on battery event API from Android SDK to record battery's changes. Trained SVM model of each volunteer approximately taking 42KB is ported to SD card of the device to predict new incoming signals. Each prototype takes about 11MB on phone's memory. Its snapshot is shown as in Figure 13.

Figure 14 shows average consumptions of two prototypes within 2.5 hours of volunteers. The method using SVM classifier and features on frequency domain consumes much energy than the remaining method in average.

Table 3: Accuracies in single and multiple-subject prediction types.

| Data type | Bicycling | Down-stair | Jogging | Up-stair | Walking |
|---|---|---|---|---|---|
| Single | 95.32% | 91.1% | 94.55% | 92.3% | 95.2% |
| Multiple | 86.36% | 72.2% | 83.42% | 76.44% | 85.12% |

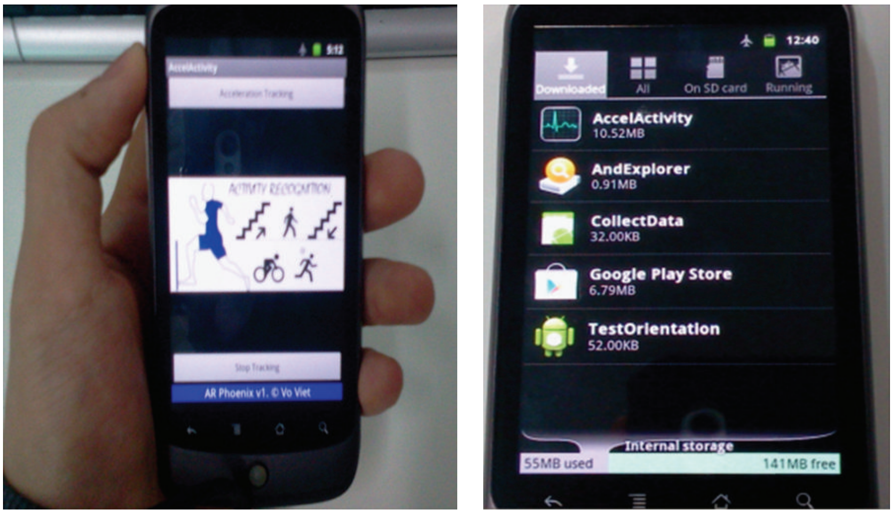

(a)

(b)

Figure 13: The implementation on HTC Nexus and its volume.

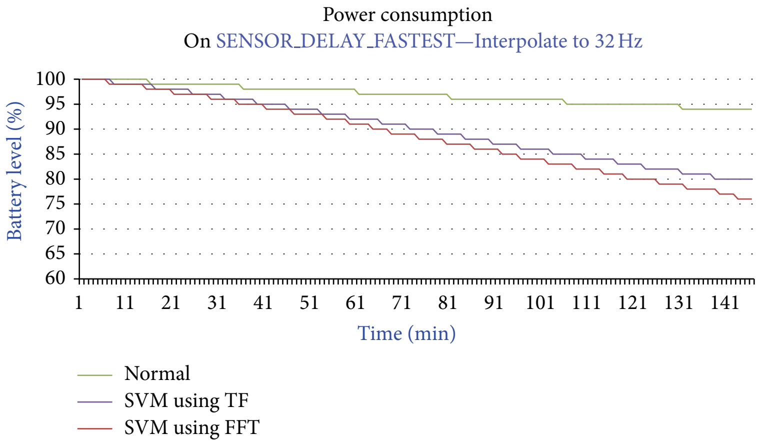

Figure 14: Battery lifetime in two prototypes and normal running.

Moreover, computational complexity on time domain is more effective than frequency domain as follows:

$$\begin{aligned} O(\mathrm{TF}) &= O(n)\,[\text{Mean}] + O(n)\,\text{Variance} + O(n)\,[\text{Energy}] \\ &\quad + O(n)\,[\text{Mobility, Complexity}] \\ &\quad + O(kn)\,[\text{Peak detection}] \quad \text{with } k \ll n \\ &= O(n), \\ O(\mathrm{FFT}) &= O(n\log n), \end{aligned} \tag{12}$$

where $n$ is total number of data points in signal, and $k$ is true peaks. Data analysis in time domain can retrieve useful information which describes characteristics of signal better than amplitude of coefficients in frequency domain. Therefore, the features on time domain are used to personalize SVM models among mobile users in next steps.

## 6. Performance of Personalization on Mobile AR System

To illustrate the performance of our algorithm, we verify the personalization algorithm with two subjects who yielded the lowest accuracy from multiple-subject prediction type

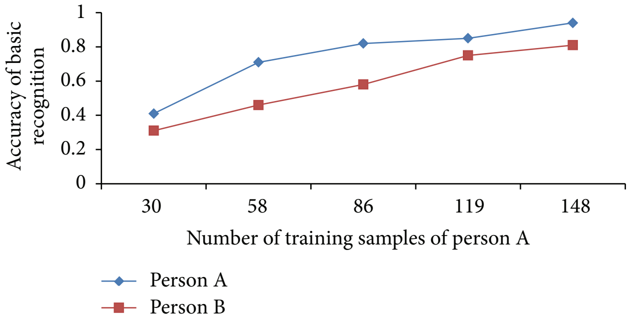

Figure 15: The impact of training samples of person A.

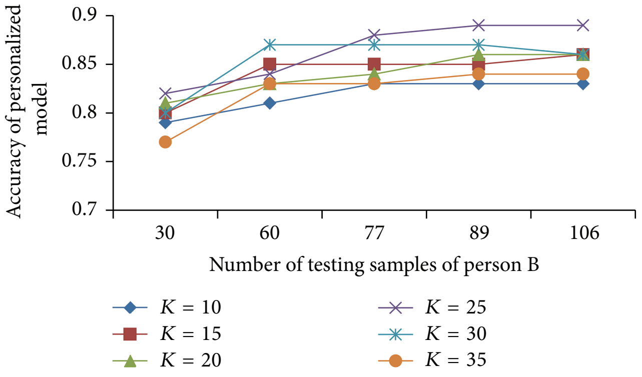

Figure 16: The impact of $K$ confident samples and testing samples in $K$-means method.

as shown in Table 2. Experiment is formed by two phases including personalizing predefined activities and measuring the efficiency of the personalized model in predicting new activities.

*6.1. Personalization in Predefined Activities.* Firstly, we measure the impact of training samples in multiple-prediction type of these two subjects. SVM model A was created by person A from total 148 samples of five activities including bicycling, downstair, upstair, jogging, and walking. In 148 training samples of person A, we divided them into five groups with different sizes corresponding to 30, 58, 86, and 148 samples. Each group is used to train a model and predict all testing samples of person A and person B, respectively. The results are shown in Figure 15.

The accuracy of the SVM model from person A increases significantly when the number of training samples varies from 30 to 86 samples. Otherwise, from 86 to 148 samples, the accuracy increases less than the previous range. In other words, with 86 training samples, we can build well a sufficient model to predict testing of person A. Accuracy of predicting all testing data of person B also increases gradually when we increase user A's training samples because the probability for successful prediction is improved when new data of person B are added more.

In order to observe the effect of $K$ confident samples used for personalizing algorithm in cases of $K$-means and $K$-medoids clustering algorithms, we used all 148 training samples of person A to predict different groups of testing data of person B, respectively. We divided testing data of person B into five groups with quantities as in 30, 60, 77, 89, and 106 samples.

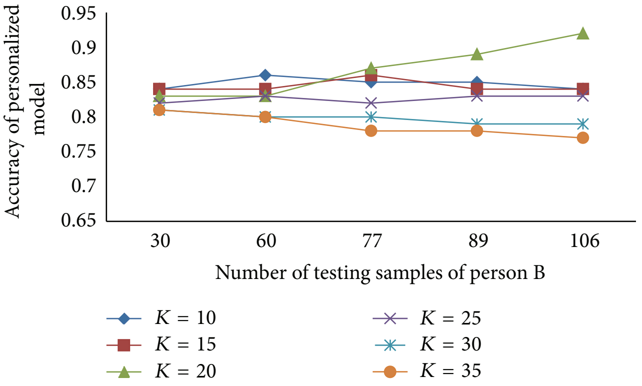

Figure 17: The impact of $K$ confident samples and testing samples in $K$-medoids method.

Table 4: Performance of $K$-means and $K$-medoids.

| Standards in measurement | Clustering method | | | |
|---|---|---|---|---|
| | $K$-means | | $K$-medoids | |
| Average accuracy improved | 8% | | 11% | |
| Confident sample size | 25 | | 20 | |
| Computational time | $O(ikn)$ | (17) | $O\left(ik(n-k)^2\right)$ | (18) |

$i$: the total number of iterations.
$k$: the total number of clusters.
$n$: the total number of samples.

Figure 16 shows the accuracies when we vary $K$ and the number of testing samples. For each $K$ case, its accuracy can converge regardless of whether $K$ is small or large when we increase testing samples. It can be explained that new testing samples of a new user are very diverse, and the probability of matching correctly to personalized model can be increased. However, the samples must perform a unique motion style of individual people in each activity. They cannot have quite difference to each other. Moreover, $K$-means algorithm of personalization process divided separately activities into different groups. These reasons made a convergence in accuracy of a person when we increase testing samples to a sufficient quantity.

At each quantity of testing samples, changing confident samples can add more noises. Thus, its accuracy can be descended. We found that a value of $K = 25$ yielded the optimal results. It can be explained that, when the value of $K$ is too small, the useful information of the new user is comparatively little. $K = 25$ is sufficient to increase 8% of accuracy compared with pure multiple-prediction type as in Figure 15.

Figure 17 represents the performance of $K$-medoids method. In contrast to the previous method, this clustering method performs stability when we vary number of testing samples. Higher accuracies compared to $K$-means method in small testing sample groups are achieved. However, when testing sample number is over a 77-sample size, it involves

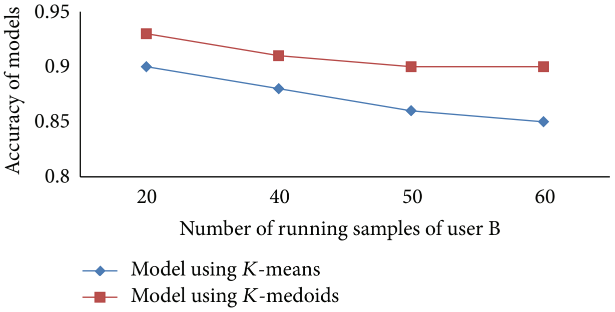

FIGURE 18: The impact of running testing samples in the models using $K$-means and $K$-medoids methods.

a converging reduction in the cases of $K$ except for the value at 20.

In fact, $K$-medoids method is more robust than $K$-means in the presence of noise and outliers, because a medoid is less influenced by outliers or other extreme values than a mean, while $k$-means perform well in processing large data sets with a discrete distribution. In cases of small testing sample groups, the model is updated by crucially correct samples when we select $K = 10$ and 15. In large testing data groups including $K = 25$, 30 and 35, the precision descended since more noises were enhanced inside. At the optimal value of $K = 20$, the accuracy of personalization process is improved up to 11 percent compared with pure multiple-prediction type as in Figure 15. Table 4 summarizes the performance of both methods. Normally, $k \ll n$ and $i \ll n$, and $K$-medoids consume more time for personalizing although an effective accuracy and an optimal quantity of confident samples are achieved.

During the test, the user-defined threshold for iteration $\Delta_{\text{Time}}$ was set as 85. However, $K$-means algorithm stopped at round $i = 25$ while this number was identified at averagely 36 for $K$-medoids algorithm. These results show an effective computational time for running real time on mobile.

*6.2. Updating New Activity in Personalized Model.* In this experiment, we use two personalized models based on $K$-means at $K = 25$ and $K$-medoids at $K = 20$, respectively. The models were personalized from all 106 testing samples on user B. To measure the effectiveness in predicting new activities, we collected new samples from new running activity on the user. Since running is different from jogging activity on velocity, and the false-positive rate of them is high.

The models are firstly trained by 40 running samples. In terms of prediction phase, a quantity of 60 samples on the activity is collected and then divided into four groups with different sizes as in 20, 40, 50, and 60 samples. From Figure 18, we could observe that

(i) the model based on $K$-medoids method performs the effective tolerance while sample size is varied;

(ii) a convergence appeared in both methods regardless of increasing testing data quantity from the size of 40 samples. Since there are many activities that need to be updated on the model, more training samples should be on-board trained to maintain an effective accuracy rate.

## 7. Conclusions

In this paper, an effective personalization algorithm that integrates SVM classification and $K$-medoids clustering method is proposed to select confident samples for updating a given AR model. The algorithm's performance is verified through recognizing predefined and new activities. An increasing accuracy of 11% is compared to nonpersonalization approach. The personalization algorithm is developed based on a basic mobile AR system that extracts time domain features from windows segmented by peaks on $Y$ axis. The effectiveness of system is compared to previous achievements in accuracy standard and another system that uses frequency domain features for energy consumption standard.

## Acknowledgment

This research was supported by Basic Science Research Program through the National Research Foundation of Korea (NRF) funded by the Ministry of Education, Science and Technology (2012-035454).

## References

[1] V. Q. Viet and D. Choi, "Energy saving in forward fall detection using mobile accelerometer," *International Journal of Distributed Systems and Technologies*, vol. 4, no. 1, pp. 78–94, 2013.

[2] M. O. Derawi, C. Nickely, P. Bours, and C. Busch, "Unobtrusive user-authentication on mobile phones using biometric gait recognition," in *Proceedings of the 6th International Conference on Intelligent Information Hiding and Multimedia Signal Processing (IIHMSP '10)*, pp. 306–311, October 2010.

[3] D. Sharma and S. Khurana, "Secure personal recognition system based on hashes keys," *International Journal of Advanced Science and Technology*, vol. 47, 2012.

[4] D. Choujaa and N. Dulay, "Activity recognition using mobile phones: achievements, challenges, and recommendations," How To Do Good Research in Activity Recognition: experimental methodology, performance evaluation and reproducibility, Workshop in conjunction with Pervasive, 2010.

[5] M. Khan, S. Ahamed, M. Rahman, and R. O. Smith, "A feature extraction method for realtime human activity recognition on cell phones," in *Proceedings of International Symposium on Quality of Life Technology*, 2011.

[6] S. Das, L. Green, B. Perez, and M. Murphy, "Detecting user activities using the accelerometer on android smartphones," The Team for Research in Ubiquitous Secure Technology, TRUST-REU Carnefie Mellon University, 2010.

[7] V. Q. Viet, H. M. Thang, and D. Choi, "Balancing precision and battery drain in activity recognition on mobile phone," in *Proceeding of 18th IEEE International Conference on Parallel and Distributed System*, pp. 712–713, 2012.

[8] V. Q. Viet, H. M. Thang, and D. Choi, "Adaptive energy-saving strategy for activity recognition on mobile phone," in *Proceeding of 12th IEEE International Symposium on Signal Processing and Information Technology*, 2012.

[9] J. A. Hartigan and M. A. Wong, "Algorithm AS 136: a k-means clustering algorithm," *Journal of the Royal Statistical Society C*, vol. 28, no. 1, pp. 100–108, 1979.

[10] H.-S. Park and C.-H. Jun, "A simple and fast algorithm for K-medoids clustering," *Expert Systems with Applications*, vol. 36, no. 2, pp. 3336–3341, 2009.

[11] J. Kwapisz, G. Weiss, and S. A. Moore, "Activity recogntion using cell phone accelerometer," in *Proceeding of ACM SIGKDD Conference of Knowledge Discovery and Data Mining*, pp. 74–82, 2010.

[12] B. Nham, K. Siangliulue, and S. Yeung, "Predicting Mode of Transport form iPhone Accelerometer Data," Stanford University class project, 2008, http://cs229.stanford.edu/proj2008/NhamSiangliulueYeung-PredictingModeOfTransportFromIphoneAccelerometerData.pdf.

[13] J. B. Gomes, S. Krishnaswamy, M. M. Gaber, P. A. C. Sousa, and E. Menasalvas, "MARS: a personalised mobile activity recognition system," in *Proceedings of the IEEE International Conference on Mobile Data Management*, 2012.

[14] S. J. Pan and Q. Yang, "A survey on transfer learning," *IEEE Transactions on Knowledge and Data Engineering*, vol. 22, no. 10, pp. 1345–1359, 2010.

[15] Z. Zhao, Y. Chen, J. Liu, Z. Shen, and M. Liu, "Cross-people mobile-phone based activity recognition," in *Proceedings of 22nd International Joint Conference on Artifica Intelligence*, pp. 2545–2550, 2011.

[16] Y. Xue and L. Jin, "A naturalistic 3D acceleration-based activity dataset & benchmark evaluations," in *Proceedings of the IEEE International Conference on Systems, Man and Cybernetics (SMC '10)*, pp. 4081–4085, October 2010.

[17] Y. Fujiki, "iPhone as a physical activity measurement platform," in *Proceedings of the 28th Annual ACM CHI Conference on Human Factors in Computing Systems*, pp. 4315–4320, April 2010.

[18] B. Hjorth, "EEG analysis based on time domain properties," *Electroencephalography and Clinical Neurophysiology*, vol. 29, no. 3, pp. 306–310, 1970.

[19] K. Ansari-Asl, G. Chanel, and T. Pan, "A channel selection method for EEG classification in emotion assessment based on synchronzation likelihood," in *Proceeding of 15th European Signal Processing Conference (EUSIPCO '07)*, pp. 1241–1245, 2007.

[20] M. W. Whittle, *Gait Analysis an Introduction*, 4th edition, 2007.

[21] T. Velmurugan and T. Santhanam, "A Survey of partition based clustering algorithms in data mining: an experimental approach," *Information Technology Journal*, vol. 10, no. 3, pp. 478–484, 2011.

Journal of
Engineering

The Scientific World Journal

International Journal of
Rotating Machinery

Journal of
Sensors

International Journal of
Distributed Sensor Networks

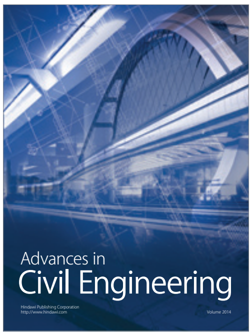
Advances in
Civil Engineering

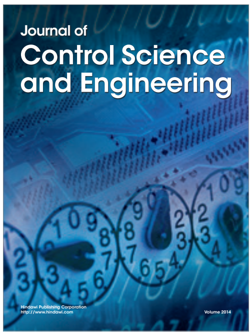
Journal of
Control Science and Engineering

Journal of
Robotics

Journal of
Electrical and Computer Engineering

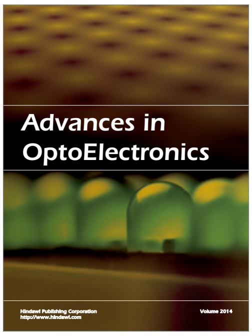
Advances in
OptoElectronics

VLSI Design

International Journal of
Navigation and Observation

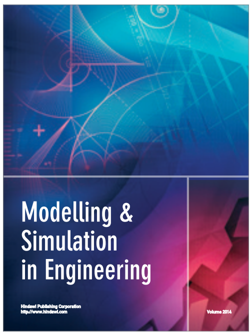
Modelling &
Simulation
in Engineering

International Journal of
Aerospace Engineering

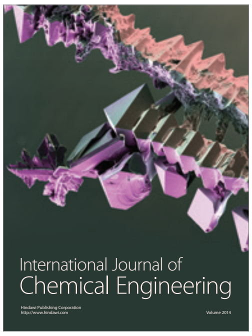
International Journal of
Chemical Engineering

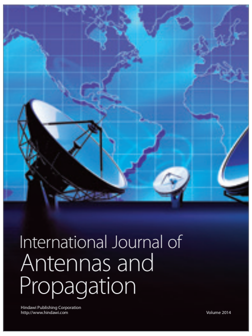
International Journal of
Antennas and Propagation

Active and Passive
Electronic Components

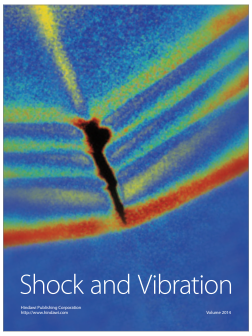
Shock and Vibration

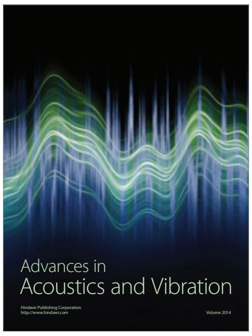
Advances in
Acoustics and Vibration